Journal of Hydrology (2007) 338, 73–84

available at www.sciencedirect.com

ScienceDirect

journal homepage: www.elsevier.com/locate/jhydrol

Response of sloping unconfined aquifer to stage changes in adjacent stream II. Applications

Antonis D. Koussis *, Evangelos Akylas, Katerina Mazi

Institute for Environmental Research and Sustainable Development, National Observatory of Athens, I. Metaxa and Vassileos Pavlou, GR-15236 Palea Penteli, Athens, Greece

Received 31 July 2006; received in revised form 12 February 2007; accepted 19 February 2007

KEYWORDS
Bank storage;
Boussinesq equation;
Convolution;
Sloping aquifer;
Stream–aquifer interaction;
Transient flow

Summary We convolve the system response functions of the linearised 1D equation of Boussinesq (extended for slope, Dupuit approximation) derived in the companion paper of Akylas and Koussis [Akylas, E., Koussis, A.D., (submitted for publication). Response of sloping unconfined aquifer to stage changes in adjacent stream: I. Theoretical analysis and derivation of system response functions, J. Hydrol] and develop solutions for the interaction of a fully penetrating stream with a sloping unconfined aquifer, taking also into account a low-conductivity streambed layer. These solutions give the aquifer stage and flow rate, the flow exchange rate at the stream–aquifer interface and the exchanged water volumes (bank storage/release). The solutions are analytical, when the flow-inducing stream stage variations are common functions; otherwise, the convolution integral is evaluated numerically. Responses are compared for aquifers on positive, negative and zero base slopes to a wave-like change in the stage of the stream. Analytical and numerical convolution-derived solutions are used to model the interaction of Cedar River and its adjacent unconfined aquifer near Cedar Rapids, Iowa. In the model, the aquifer base is taken to be horizontal or inclined and the streambed clogged by a low-conductivity sediment layer; the model is verified against data not used in the calibration and is found to perform very well.

Introduction: development of solutions by convolution

We develop convolution-based solutions to the stream–aquifer interaction problem for arbitrary stream forcing, using the system response functions (SRF) derived in the

DOI of original article: 10.1016/j.jhydrol.2007.02.021.
* Corresponding author. Tel.: +30 210 810 9125, fax: +30 210 810 3236.
E-mail address: akoussis@env.meteo.noa.gr (A.D. Koussis).

0022-1694/$ - see front matter © 2007 Elsevier B.V. All rights reserved.
doi:10.1016/j.jhydrol.2007.02.030

Nomenclature

Notation
Definition of symbols, with dimension (L, length; T, time)

a	solution parameter entailing the ratio of velocity to diffusion coefficient [L^{-1}]
b_s	thickness of low-conductivity sediment layer in streambed [L]
D	diffusion coefficient of aquifer [L^2T^{-1}]
$f(\omega t)$	periodic part of forcing function [−]
h	height of water column measured normal to the bed, depth of aquifer [L]
h_0	depth of linearisation of the aquifer [L]
h_{stream}	function of the stream depth hydrograph
K	hydraulic conductivity of aquifer [$L\,T^{-1}$]
K_s	hydraulic conductivity of sediment streambed layer [$L\,T^{-1}$]
l	streambed leakance [L]
L	length of aquifer [L]
n	drainable porosity (specific yield) of aquifer [−]
q	aquifer discharge per unit width [$L^2\,T^{-1}$]
r	recharge rate [$L\,T^{-1}$]
s_v	poles in the power series development of analytic functions (theorem of residua) [T^{-1}]
S	slope of aquifer basis, defined as sin φ [−]
t	time [T]
t_c	time of crest of the Cooper-and-Rorabough stream hydrograph [T]
T	period of periodic forcing [T]
u	system response function [T^{-1}]
vol	volume of water exchanged with aquifer, per unit stream length [$L^2\,T^{-1}$]
V	gravity-driven (kinematic wave) linear pore velocity of aquifer, KS/n [$L\,T^{-1}$]
X	distance measured along the aquifer base [L]
y	depth at stream−aquifer interface [L]
z_v	v th root of the equation $\tan z = f(z, a, l, L)$ [−]
α	effective amplitude
$\alpha_v(x)$	space-dependent part of the system response function [−]
δ	parameter in exponential function of stream flood hydrograph [T^{-1}]
η_v	function of parameters in expression for the vth residuum, η_v (a, l, L, z_v, y)
$\xi_v(x)$	spatial function in expression for the vth residuum [−]
τ	dummy variable of integration over time [T]
φ	inclination angle of aquifer base against the horizontal [−]
ω	frequency of wave forcing function [T^{-1}].

companion paper of Akylas and Koussis, henceforth A & K (in review). The SRF of the linearised 1D Boussinesq equation is based on the Dupuit−Forchheimer theory (hydrostatic pressure in the water column) and the stream is assumed to completely penetrate a sloping aquifer. We also apply the convolution solutions to a field case, demonstrating its utility in hydrologic practice.

The assumption of system linearity allows superposition of solutions. This fundamental principle, expressed either by the convolution integral or numerically as the sum of responses to discrete inputs, is well established in hydrology, mainly in surface water applications. Barlow et al. (2000), among others, have applied numerical convolution to the stream−aquifer interaction problem. Convolving the SRF, $u(x,t)$, with the arbitrary forcing function $h_{stream}(\tau)$ above the initial stream stage yields solutions relative to the initial condition in the aquifer

$$h(x,t) = \int_0^t h_{stream}(\tau)u(x,t-\tau)\mathrm{d}\tau = \int_0^t h_{stream}(t-\tau)u(x,\tau)\mathrm{d}\tau. \tag{1}$$

The following SRF's for the stream−aquifer interaction are given in the companion paper of A & K (in review): in the absence of a sediment streambed layer, Eq. (38) for a sloping aquifer and Eq. (53) for a horizontal aquifer; in the presence of a sediment layer, Eq. (32b) for a sloping aquifer [residua defined by the general expression Eq. (31)] and Eq. (61) for a horizontal aquifer. In the general case, i.e., with $u(x,t)$ given by Eq. (32b), Eq. (1) (see Notation), yields

$$h(x,t) = \sum_{v=1}^{\infty} \eta_v(a,l,L,z_v,y=1)s_v\xi_v(x)\mathrm{e}^{s_v t} \times \int_0^t h_{stream}(\tau)\mathrm{e}^{s_v t}\,\mathrm{d}\tau. \tag{2}$$

The numerical evaluation of the convolution integral opens up wide applications generality for arbitrary excitations; however, fine discretisation may be required for accuracy, especially for the seepage rate, which involves numerical differentiation. For example, Barlow et al. (2000) used numerical convolution with $\Delta t = 0.01$ day, yet the computed seepage rate did not match the analytical results of Cooper and Rorabough (1963) [C & R (1963), henceforth] very well, particularly close to extremes. In contrast, an analytical solution is free of such limitations and preferable, if the signal can be fitted by analytical expressions such as periodic forcing function (excitation is relative to the initial stage) (e.g., C & R (1963))

$$h_{stream}(0 \leqslant t \leqslant T) = A\exp(-\delta t)f(\omega t) \quad \text{and} \quad h_{stream}(t > T) = 0, \tag{3}$$

in which A is the nominal amplitude of a wave with frequency ω (period $T = 2\pi/\omega$) and δ a parameter controlling the asymmetry of the signal ($\delta = 0$ for a symmetric hydrograph). Analytical convolution, Eq. (2), is indeed feasible for a large class of forcing functions, although the output expressions can be lengthy; we give such examples in the following.

Some analytical solutions by convolution

We start with the simpler analytical expressions derived when a sediment bed layer is ignored, however, the general case will be used in the numerical examples. Thus Eq. (2), with Eq. (38) in A & K (in review) for a sloping aquifer base, yields

$$\frac{h(x,t)}{\frac{2D}{L^2}e^{-\frac{Sx}{2h_0\cos\varphi}}} = \sum_{v=1}^{\infty}\frac{z_v\sin\left(\frac{z_v x}{L}\right)}{1-\frac{aL}{z_v^2+a^2L^2}}\int_0^t h(0,\tau)e^{-\frac{D}{L^2}\left(z_v^2+a^2L^2\right)(t-\tau)}d\tau$$
$$= \sum_{v=1}^{\infty}\alpha_v(x)e^{-s_v t}\int_0^t h(0,\tau)e^{s_v\tau}\,d\tau, \qquad (4)$$

$$\alpha_v(x) = z_v\sin\left(\frac{z_v x}{L}\right)\left(1-\frac{aL}{z_v^2+a^2L^2}\right)^{-1},$$

$$s_v = -D\left(\frac{z_v^2}{L^2}+\frac{V^2}{4D^2}\right). \qquad (5)$$

The flow rate $q = -K(hS + h_0\partial h/\partial x)$, Eq. (4) of A & K (in review), becomes with Eqs. 4, 5

$$q(x,t) = -\frac{KD}{L^2}e^{-\frac{Sx}{2h_0\cos\varphi}}\sum_{v=1}^{\infty}\left[S\alpha_v(x)+2h_0\cos\varphi\frac{d\alpha_v(x)}{dx}\right]e^{s_v t}$$
$$\times\int_0^t h(0,\tau)e^{-s_v t}\,d\tau. \qquad (6)$$

The discontinuity at $x = 0$ does not allow to evaluate the stream–aquifer flow exchange rate $q(x = 0, t)$ by Eq. (6), therefore bank storage should be computed from the depth profiles.

The solutions for a horizontal and for a sloping aquifer differ only in the values of α_v and s_v defined by the roots z_v; these are periodical for a horizontal aquifer, Eq. (47) in A & K (in review), and calculated iteratively when the base of the aquifer is sloping. For example, for the C & R (1963) forcing function in Eq. (3), $f(\omega t) = 0.5(1-\cos\omega t)$, with effective amplitude $\alpha = A\exp(-\delta t_c)$, $t_c = 2\omega^{-1}\arctan(\omega/\delta)$, the convolution integral yields for $t \leqslant T$:

$$h(x, t\leqslant t_p) = A\frac{D}{L^2}e^{\frac{-Sx}{2h_0\cos\varphi}}\sum_{v=1}^{\infty}\alpha_v(x)e^{s_v t}\int_0^t(1-\cos\omega\tau)e^{-(\delta+s_v)\tau}d\tau$$
$$= A\frac{Kh_0\cos\varphi}{nL^2}e^{\frac{-Sx}{2h_0\cos\varphi}}\sum_{v=1}^{\infty}\alpha_v(x)\frac{-e^{-\delta t}}{s_v+\delta}$$
$$\times\left[1-e^{(s_v+\delta)t}-\frac{\cos\omega t-[\omega/(s_v+\delta)]\sin\omega t-e^{(s_v+\delta)t}}{1+\omega^2/(s_v+\delta)^2}\right]. \qquad (7)$$

Solutions for $t > T$ are obtained by superposing two *infinite duration* signals, i.e., subtracting from Eq. (7) the response to $A\exp(-\delta t)f(\omega t)$ for $t > T(t \to t + T)$. The evolutions of exchange flow and bank storage induced by the stream transient (flood wave) are obtained from Eqs. (4) and (40) in A & K (in review), respectively, both evaluated with Eq. (7).

Evidently, other analytical responses to periodic signals can be also derived. For example, if the stream level variation is a sinusoid with phase shift θ_0, $h_{stream}(t) = Ae^{-\delta t}\sin(\omega t+\theta_0)$ [or equivalently, $h_{stream}(t) = e^{-\delta t}(A_1\sin\omega t + A_2\cos\omega t)$, since $\tan\theta_0 = A_2/A_1$ and $A = (A+_1^2 + A_2^2)^{1/2}$], the solution is given by

$$h(x,t) = \frac{2D}{L^2}e^{\frac{-Sx}{2h_0\cos\varphi}}\sum_{v=1}^{\infty}\alpha_v(x)\frac{-(s_v+\delta)^{-1}}{1+\omega^2/(s_v+\delta)^2}$$
$$\times\left\{Ae^{-(s_v+\delta)t}[\sin(\omega t+\theta_0)+[\omega/(s_v+\delta)]\sin(\omega t-\theta_0)]\right.$$
$$\left.-A_1\omega/(s_v+\delta)-A_2\right\}. \qquad (8)$$

Next, we re-examine the interaction of a stream with a horizontal aquifer using as flood hydrograph $h_{stream}(t) = Ae^{-\delta t}0.5(1-\cos\omega t)$ (C & R, 1963). For $S = 0$, $a = 0$ and $\alpha_v = z_v\sin(z_v x/L)$, $d\alpha_v/dx = (z_v^2/L)\cos(z_v x/L)$, $s_v = -(D/L^2)z_v^2$ and $z_v = (2v-1)\pi/2$; for a symmetric wave ($\delta = 0$), the aquifer stage, flow rate and bank storage are, then, respectively:

$$h(x, t\leqslant t_p) = A\sum_{v=1}^{\infty}\left[(2v-1)\frac{\pi}{2}\right]^{-1}\sin\left[(2v-1)\frac{\pi}{2}\frac{x}{L}\right]$$
$$\times\left[1-e^{s_v t}-\frac{\cos\omega t-(\omega/s_v)\sin\omega t-e^{s_v t}}{1+\omega^2/s_v^2}\right], \qquad (9)$$

$$q(x, t\leqslant t_p) = -Kh_0\frac{A}{L}\sum_{v=1}^{\infty}\cos\left[(2v-1)\frac{\pi}{2}\frac{x}{L}\right]$$
$$\times\left[1-e^{s_v t}-\frac{\cos\omega t-(\omega/s_v)\sin\omega t-e^{s_v t}}{1+\omega^2/s_v^2}\right], \qquad (10)$$

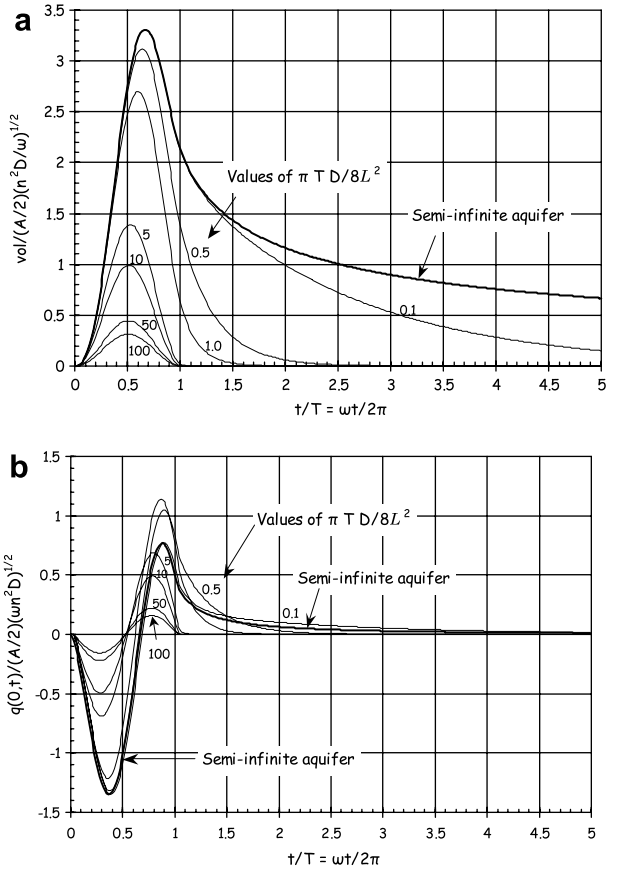

Figure 1 Bank storage (a) and seepage rate at the stream–aquifer interface (b) caused by the passage of a flood wave, with $h_{stream}(t) = 0.5A(1-\cos\omega t)$ above the initial stage; the aquifer is horizontal.

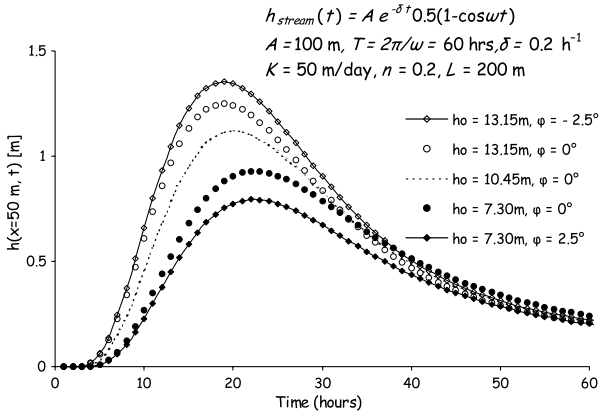

Figure 2 Comparison of hydrographs for aquifer base slopes $\varphi = +2.5°$, $-2.5°$ and $0°$.

$$\mathrm{vol}(t \leqslant t_p) = -Kh_0\frac{A}{L} \times \sum_{v=1}^{\infty}\left[t + \frac{1}{s_v}(1-\mathrm{e}^{-s_v t}) - \frac{\omega^{-1}\sin\omega t + s_v^{-1}\cos\omega t - s_v^{-1}\mathrm{e}^{s_v t}}{1+\omega^2/s_v^2}\right]. \quad (11)$$

The results of Eqs. (9)—(11) agree numerically with those of C & R (1963). The curve parameter $\pi TD/8L^2$ distinguishes the solution graphs in Fig. 1; that ratio relates the wave period T to L^2/D, a characteristic time proportional to the aquifer's *diffusive* time scale (Crank, 1975).

The influence of the slope on the aquifer response is assessed by a comparative study. The parameters of the aquifer are L = 200 m, K = 50 m/day, n = 0.2 and $\varphi = 0°, \pm 2.5°$. In the C & R stream variation $h_{\mathrm{stream}}(t) = Ae^{-\delta t}0.5(1-\cos\omega t)$ above the initial depth h_i = 8.75 m, A = 100 m, $T = 2\pi/\omega$ = 60 h and δ = 0.2 h^{-1}; the signal's amplitude is $\alpha \approx 3.4$ m. In this example, h_0 is estimated by Eq. (16) of A & K (in review) with $y = h_i + \alpha/2$ = 10.45 m, giving $h_0\cos\varphi$ = 7.30 m for $\varphi = 2.5°$ and 13.15 m for $\varphi = -2.5°$; the comparison remains however unaffected by the specific h_0-values, as long as these are chosen consistently. A more detailed discussion on the optimal linearisation depth is reserved for the field case below.

Fig. 2 shows depths for the aquifers on a sloping base, and the hydrograph for $\varphi = 0°$ and h_0 = 10.45 m as reference. Expectedly, the hydrographs of the inclined aquifers envelop that of the horizontal aquifer; the relative difference is greater between the cases $\varphi = 2.5°$ and $\varphi = 0°$ (and increases with distance from the stream). This comparison indicates also that computing even with $\varphi = 0°$ and h_0 = 7.30 m or 13.15 m yields hydrographs that still approximate crudely their slope-consistent counterparts. The situation remains qualitatively unaltered for K in the range of 10—100 m/day (results not shown).

Field application

Motivation

The water exchange between a channel and its near-bank zones is crucial to the ecological status of streams, to stream-restoration and to riparian management (Sophocleous, 2002). The scale of the system of interest falls in the range of local flow systems of the classification of Tóth (1963). Addressing the aforementioned problems quantitatively requires that the stream—aquifer system's hydraulic parameters be defined through field tests. The parameter estimation is more reliable when natural or artificial stream stage variations cause the aquifer responses, compared to equal duration pumping tests, because the range of influence of such flooding tests is greater. The estimation of the hydraulic parameters from measured head responses of the aquifer can be based on analytical solutions (flow in a plane perpendicular to the stream) such as the 2D model of Moench and Barlow (2000) and the 1D model presented here, or on a numerical model, as e.g. Rötting's et al. (2006) comprehensive characterisation of the aquifer next to the Agrio River, Spain (3D, including pumping tests and geostatistical inversion).

General setting and conceptual model framework of the application site

The new solution is applied to the site of the Cedar River and its adjacent unconfined aquifer near Cedar Rapids, Iowa shown in Fig. 3a. To model this case, Barlow et al. (2000) convolved numerically the stream hydrograph with a 2D SRF derived by Laplace transforms and inverted numerically by the Stehfest algorithm; that solution considers head variations in the vertical, but ignores the aquifer slope (horizontal base). A theoretical comparison of the 2D and 1D models follows in the concluding section. The simplified hydro-geological section of the site and its schematisation for our application are shown in Fig. 3b. The alluvial aquifer consists of glacio-fluvial sediments of coarse- to fine-grained sands and silty clayey sands fining-upward; it thins laterally, is underlain by fairly dense glacial till and carbonate bedrock and is bounded laterally by till-covered uplands at ~1310 ft (~400 m) from the stream bank.

The hydraulic connection between stream and aquifer is evident by the simultaneous variation of the water level in the partially penetrating wells near the stream bank and in the river as shown in Fig. 4. A half-day variation of over 4 ft in stream stage occurred at the site in October—Novemeber 1989, when water was released rapidly from an upstream dam, after a dry-weather period that established base flow conditions. That release caused the levels in the wells to fluctuate about 2.3—1 ft. The cross-section of Cedar River at the site is lined by a thin layer b_s of sediments of lower conductivity K_s and penetrates only ca 20% of the saturated thickness of the aquifer; in the model, however, the stream is assumed to penetrate the (homogeneous) aquifer fully.

The aquifer is modelled as inclined and horizontal and its response computed by numerical convolution; an analytical solution is also given, after fitting Eq. (3) to the stream hydrograph. Model calibration is based on the aquifer conditions caused by the rapid transient due to the aforementioned sudden water release from an upstream dam in October—November 1989. We test the calibrated model (validation) by simulating the aquifer response to the variation of the stage of Cedar River at the study site over approximately one month (March—April 1990).

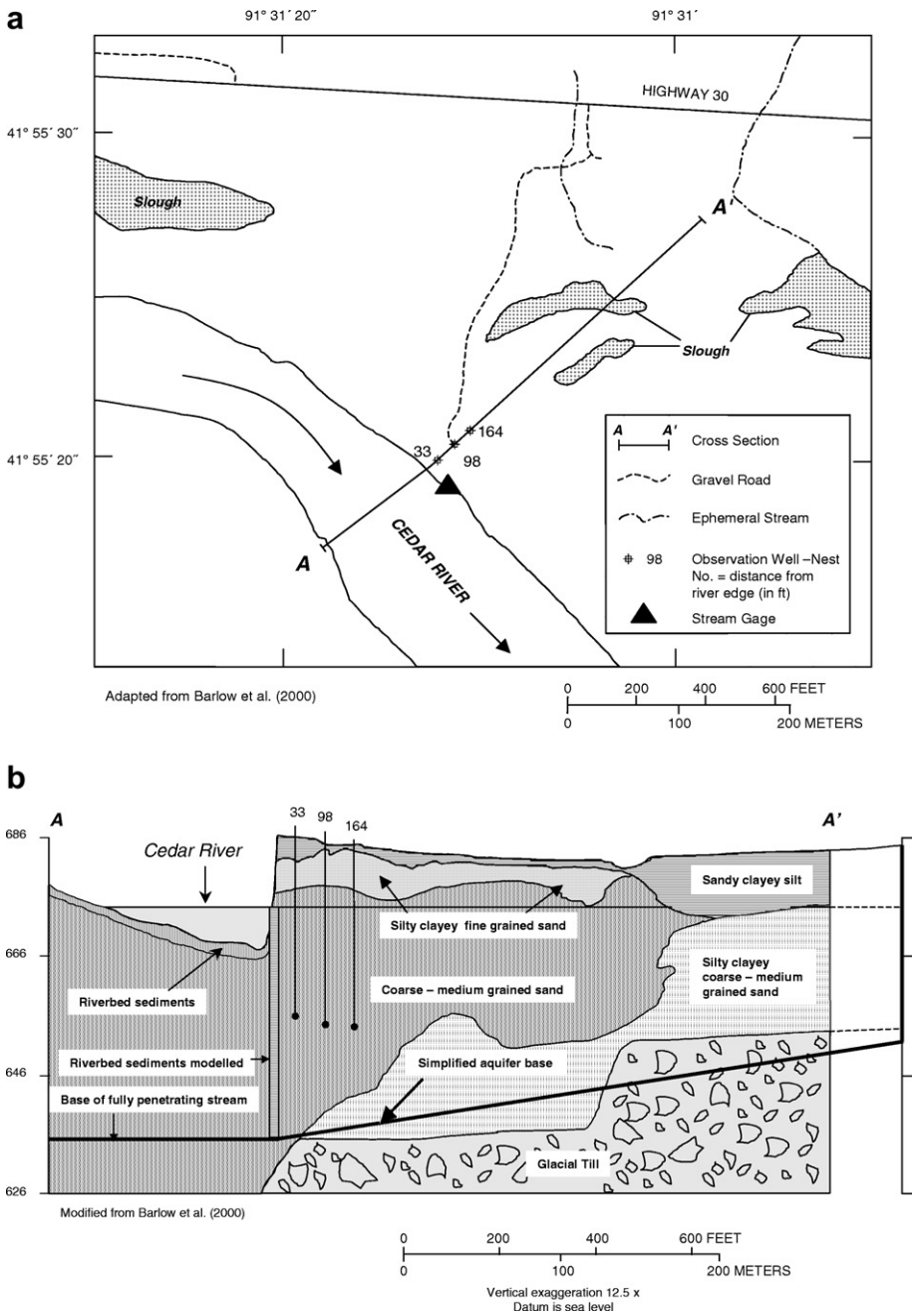

Figure 3 (a) Location of the geologic section of the Cedar River study site near Cedar Rapids, Iowa, USA. (b) Simplified geologic section of the site and schematisation for model application.

The model of the aquifer on an inclined base is conceptualised based on information from Squillace (1996). The approximate location of the glacial till bedrock shown in the geologic section of Fig. 3b is extended linearly to the distance $x \approx 1310$ ft ($\sim$400 m). In Figs. 1 and 3 of Squillace (1996), the aquifer thins laterally from a maximum alluvium thickness of about 50 ft (15.25 m) underneath the river. The inclined straight baseline in Fig. 3b, sloping with $S = \sin\varphi \approx 0.0122 (\varphi \approx 0.7°)$, approximates the irregular aquifer base and defines the aquifer base in our model. As Squillace (1996) notes, the glacial till is a valid no-flow base because its estimated hydraulic conductivity is at least 10^5 times less than that of the most permeable overlying unit.

In determining the linearisation level, we recall that h_0 is a mean depth about which the aquifer depths vary; for this reason, the h_0-values must reflect the size and the transience of the signal. For example, in the case of a pulse of size y, we may not simply use the estimate of Eq. (16) in A & K (in review) [steady flow, $h(0) = h_{is} + y/2$], without considering the pulse duration. That estimate may be a good approximation for a long-duration pulse, but is inappropriate for a pulse of short duration. In the latter case, the flow in the aquifer will be far from steady state and the water

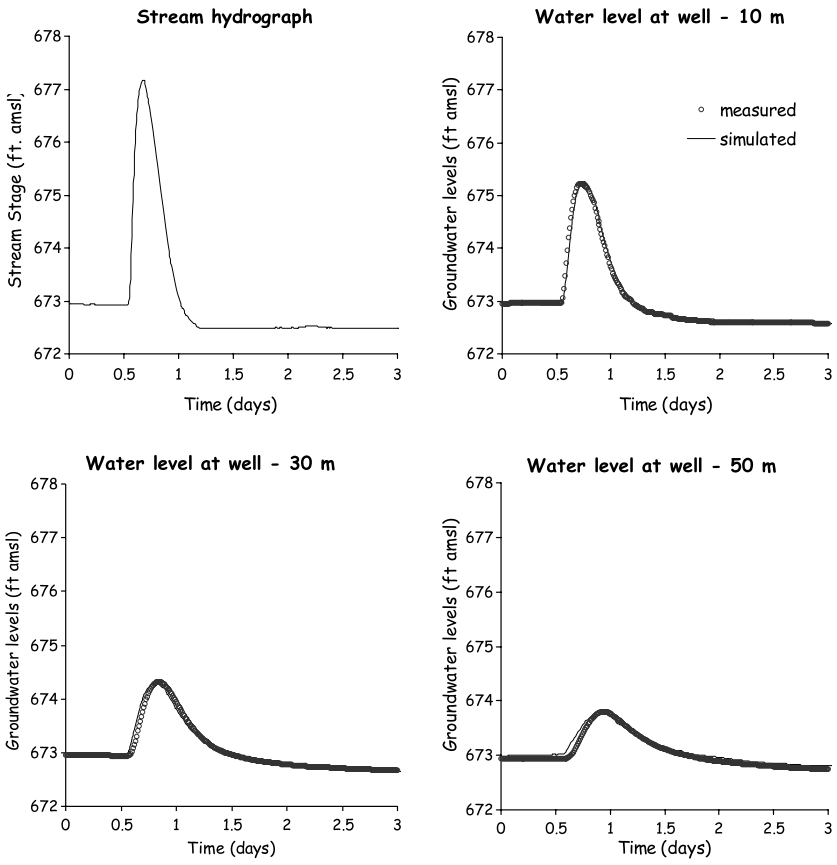

Figure 4 Stream hydrograph and variation of the water level in the partially penetrating wells near the stream bank for the October–November 1989 event and model calibration results.

level will rise far less, on average, as high-frequency signals attenuate strongly.

The dependence of a periodic input's attenuation on the frequency is seen readily from Eq. (9) (horizontal aquifer). For a low-frequency signal ($\omega \to 0$), the terms in the last bracket give $(1 - \cos\omega t)$ and, as the series converges to 1/2, Eq. (9) reproduces the input. In contrast, high-frequency signals suffer attenuation; the last bracket gives $1 - \exp(-s_v t)$ and each series term is multiplied by $\exp(-s_v t)$. In order to characterise the signal frequency as high or low, we relate it to the aquifer's *diffusive* response time at distance x from the stream that is proportional to x^2/D (Crank, 1975).

Based on the data presented immediately below, the aquifer's *diffusive* response time is at $x = L = 400$ m proportional to $L^2/D \approx (400)^2/(100 \times 10/0.2) = 32$ days. On the other hand, the October–November 1989 hydrographs show the main signal to be a high-frequency transient (period $T \approx 1$ day) that attenuates strongly, without significantly disturbing the initial flow conditions in the aquifer; e.g., the 4-ft stream amplitude causes less than 1-ft rise in the third monitoring well, at $x_{w3} \sim 50$ m. For this transient therefore, it is reasonable to assume for the linearisation depth a value slightly higher than the initial mean depth of the aquifer, say $h_0 = 9.75$ m.

Model calibration

A note on calibration parameters is appropriate before starting the modelling task. In the model version of the horizontal aquifer, performance is controlled by the *diffusivity* $D = Kh_0\cos\varphi/n$ and by the *leakance* $l = (K/K_s)b_s$; if the aquifer base is inclined, the slope S (via $a = -V/2D$; $V = KS/n$) must be also added. Of course, these parameter groups appear in the relevant SRF and in the governing equation and the boundary conditions. Barlow et al. (2000) calibrated the aquifer parameters as follows: specific yield $n = 0.2$, horizontal hydraulic conductivity $K_x = 309$ ft/day ≈ 94 m/day and also $K_z/K_x = 0.2$, while the initial thickness of the aquifer was taken as 30 ft (9.15 m); this last specification fixes the elevation of the aquifer base, which they took as horizontal. For the streambed layer, Barlow et al. (2000) adopted the values of the calibrated numerical model of Squillace (1996), $b_s = 1.6$ ft (0.5 m) and $K_s = 16$ ft/day (4.9 m/day), which give the leakance value $l = 31$ ft (9.4 m).

Because calibration of multi-parameter models is a tedious task, special codes have been designed for this purpose. These are optimisation codes that vary the parameter values systematically in a process that minimises an objective function such as the root-mean-squared-error between the model output and the measured signal. Graphical methods have been devised for the case of two parameters, but calibration of even a three-parameter model is complex. Having the benefit of the modelling studies of Squillace (1996) and of Barlow et al. (2000), we may approach the calibration heuristically. We proceed to bracket the search space of the three composite parameters, diffusivity $D = K\,h_0\cos\varphi/n$, streambed leakance $l = (K/K_s)b_s$ and

gravity-driven pore velocity $V = KS/n$, by estimating the quasi-observable aquifer parameters b_s, h_0, K, (the values of D, l and V are difficult to bracket otherwise). This approach allows determining the six individual parameters (K, K_s, b_s, n, h_0, S), since, obviously, these cannot be specified uniquely from the values of the three composite parameters.

As already mentioned, we fix the slope of the aquifer base at $S = 0.0122$; we furthermore choose, as in the previous studies, $n = 0.2$ for the aquifer's specific yield and $K_s = 16$ ft/day (4.9 m/day). We then use the information on the hydraulic conductivity given by Squillace (1996) to estimate K of the *equivalent homogeneous* aquifer on the inclined base. Assuming nearly horizontal flow, the K-value is estimated from the weighted average of the contributing layers evaluated at various vertical sections, e.g., $K_{|x=0} \approx 94$ m/day, $K_{|x\,=\,100m} \approx 75$ m/day and $K_{|x\,=\,200m} \approx 70$ m/day. Since the calibration is based on data from monitoring wells near the river, where the aquifer consists largely of the two most conductive layers, the calibrated K-value can be expected to be fairly high, ~85 m/day, say (but not 94 m/day, as the flow is influenced by the entire aquifer and K represents average conditions). In addition, the value of the linearisation depth has been already estimated as $h_0 \approx 9.75$ m. Thus, at the start of the optimisation, the values of the composite parameters are: $l = 9.4$ m from the earlier studies, $D = Kh_0 \cos\varphi / n = 85\ \text{m/day} \times 9.75/0.2 \approx 4150\ \text{m}^2/\text{day}$, and $V = K \sin\varphi / n = 85\ \text{m/day} \times 0.0122/0.2 = 5.2$ m/day.

The strategy for the use of the monitoring data is as follows. The sediment bed layer influences model results especially close to the stream, therefore the observations of the first monitoring well may be relevant for optimising l, and can be certainly used to obtain a first estimate of the leakance. Yet these data may be less suitable for the calibration of the aquifer parameters, as the first monitoring well is located only $x_{w1} \sim 10$ m from the stream bank, which is also less than $1.5h_0 \approx 15$ m, the distance estimated by Hantush (1965) as minimal for the influence of the partial stream penetration to be small. The data of the second monitoring well, $x_{w2} \approx 30$ m, are considered most relevant in the overall calibration and determinant for the aquifer parameters, as the hydrograph at the third well is defined less sharply and hence less weight is placed on matching that hydrograph.

The leakance was first optimised roughly at $l = 11.6$ m, based on the data at the first well and for $D = 4150\ \text{m}^2/\text{day}$ and $V = 5.2$ m/day (the value of b_s impacts the aquifer length between the stream and the wells, but it practically affects only the results at the near-stream well, $x_{w1} \sim 10$ m). However, the data at the second well showed that $l = 11.6$ m was too large a leakance value. Therefore, keeping the aquifer diffusivity and the gravity-driven pore velocity at their initial values, the leakance was re-optimised on the hydrograph at the second well, obtaining $l = 10.9$ m. We refined this set by varying D, l and V systematically over small ranges, aiming mainly at achieving optimal model performance at the second well, but paying also attention to good fidelity at the other two wells. In summary, the model predictions should agree generally well with all field observations, but especially at the second monitoring well.

It is also worth noting that the different initial water levels at the monitoring wells show that the aquifer is not at steady state initially, as assumed by the model solution. To bring the model application closer to the field conditions, we placed the zero-level 0.01 ft above the initial stage in the stream. The simulation results shown in Fig. 4 correspond to the calibrated composite parameters $V = 5.16$ m/day, $D = 4120\ \text{m}^2/\text{day}$ and $l = 10.86$ m. Maintaining $n = 0.2$ and $K_s = 4.9$ m/day from the previous studies and the geological slope estimate $S = 0.0122$ ($\varphi \approx 0.7°$) yields the remaining parameters as $K = 84.5$ m/day, $h_0 = 9.75$ m and $b_s = 0.63$ m.

The simulations are not very sensitive to the value of the velocity, which is explained by the very mild inclination of the aquifer base. This explanation is corroborated by the almost equal model performance when the aquifer base is assumed horizontal, with $h_0 = 9.3$ m and optimal composite parameters $D = 3930\ \text{m}^2/\text{day}$ and $l = 10.86$ m ($K = 84.5$ m/day and $b_s = 0.63$ m, as before). As we shall see later, ignoring the slope and modelling the aquifer as horizontal makes the calculation of bank storage also less accurate, but again only slightly so (about 4% for the maximum bank storage), because of the very mild slope of the aquifer base.

In contrast to the velocity, the leakance is quite important for the simulation of the aquifer hydrographs. The main reason for a streambed thickness different from $b_s = 0.5$ m in Squillace (1996) is the assumed complete stream penetration, versus the actual ~20%. This assumption on one hand ignores the true flow resistance, due to the longer and curving streamlines, and on the other reduces the stream–aquifer interface to ~12 m, compared to over 40 m in the model of Squillace (including the channel bottom). A lesser reason for the different b_s-values is the analytical model's hydraulic conductivity of $K = 84.5$ m/day, compared to $K_{|x=0} = 94$ m/day, the average K corresponding to the alluvial material of the row next to the stream in the MODFLOW simulation of Squillace et al. (1996).

The above arguments are in line with the opinion of Barlow et al. (2000) that the leakance may be viewed as a parameter through which not only the presence of a streambed sediment layer is taken into account, but structural model shortcomings, such as not accounting for partial stream penetration, can be moderated in the calibration. Finally, a linearisation depth value close to the initial mean depth of the aquifer is also supported by the strong dissipation of the simulated hydrographs; e.g., at $x = 100$ m and $x = 200$ m, their respective peaks are less than 1/3 ft and 1/10 ft.

Model validation

Adjustment of linearisation level

The calibrated model is validated on the data of March–April 1990. The model's depth of linearisation is adjusted to reflect the larger and much slower transient than the October–November 1989 calibration event. Its ~30-day period (see analytical study below) compares to L^2/D. This signal has an accordingly lower frequency and attenuates far less than the high-frequency calibration signal, traversing the aquifer with only modest change. The relevant h_0-value should therefore be noticeably higher than the calibrated value. On these grounds, we estimate h_0 from the

steady state aquifer profile for the peak value of the stream hydrograph and obtain $h_0 = 11.5$ m and for the corresponding aquifer diffusivity $D = 4860\ \mathrm{m}^2/\mathrm{day}$. Such an aquifer-wide based linearisation may underestimate the above-average depths in the near-stream region, but is acceptable because it has a rational basis.

Consideration of recharge

The presented solutions do not include recharge, which is reported to have taken place in the validation field case. A crude way to account for the effect of recharge r is to increase the aquifer response to the stream hydrograph by the recharge contribution rt/n (any recharge-related rise of the water level prior to the event is reflected in the initial level of the aquifer). But this rate of increase is too high, as no outflow from the aquifer is allowed, and surely this rate of rise does not continue indefinitely. It is yet apparent from their Fig. 10 that Barlow et al. (2000) adopted such a constant rate of water level rise; and this explains their choice of $r = 0.002$ ft/day, instead of 0.0034 ft/day used in the numerical model of the site by Squillace et al. (1996), and their clear overestimation of the falling limbs of the hydrographs.

A more credible approach would allow for outflow that naturally limits the rise of the water table. Conceptualising the aquifer as a linear reservoir, vol = $k\ q_{out}$ (time constant k), improves upon the aforementioned 'constant rise' recharge model. With vol = $nL\langle\Delta h\rangle$, $\langle\Delta h\rangle$ being the aquifer-wide average water level above the initial one, the reservoir's storage balance reads:

$$\mathrm{d}(vol)/\mathrm{d}t = k\mathrm{d}q_{out}/\mathrm{d}t = nL\,\mathrm{d}\langle\Delta h\rangle/\mathrm{d}t = rL - q_{out} = rL - nL\langle\Delta h\rangle/k. \quad (12)$$

Instead of $q_{out} = rL(1 - \mathrm{e}^{-t/k})$, we give as solution (asymptotic approach to steady state $\langle\Delta h_{ss}\rangle$):

$$\langle\Delta h\rangle = \langle\Delta h_{ss}\rangle(1 - \mathrm{e}^{-t/k}). \quad (13)$$

To evaluate Eq. (13), we estimate the reservoir's time constant and its steady state water level. To this end, we consider the aquifer as horizontal and bounded laterally by a stream and an impervious barrier at a distance L from the stream. The aquifer's initial uniform depth, h_i, is identical to the constant stream depth, i.e., $h(0) = h_i$. The steady state depth profile is then

$$\Delta h_{ss}(x) = h_i[1 + (r/Kh_i^2)(2Lx - x^2)]^{1/2}. \quad (14)$$

After integration over L and division by L, this profile gives the mean steady state depth in the aquifer $\langle\Delta h_{ss}\rangle$. The truncated binomial series approximation $[1 + (r/Kh_i^2)(2Lx - x^2)]^{1/2} \approx [1 + (r/2Kh_i^2)(2Lx - x^2)]$ is excellent and facilitates the integration yielding the explicit estimate of Eq. (15), which is identical to the solution of the linearised problem,

$$\langle\Delta h_{ss}\rangle = rL^2/3Kh_i. \quad (15)$$

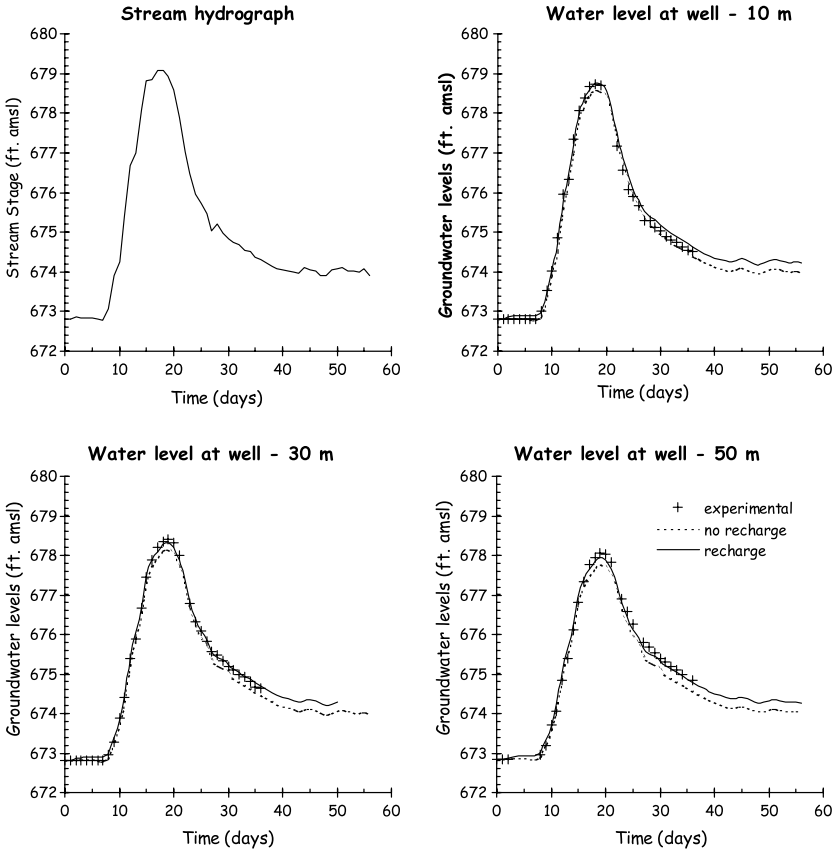

Figure 5 Stream hydrograph and variation of the water level in the partially penetrating wells near the stream bank for the March–April 1990 event and model verification results.

Applying Eq. (15) with $r = 1.2 \times 10^{-8}$ m/s (0.0034 ft/day), the recharge rate used by Squillace et al. (1996) in their numerical model of the site, and with $h_i = 9.15$ m (aquifer taken as horizontal) gives $\langle \Delta h_{ss} \rangle \approx 0.07$ m. Then, setting $k = (\text{vol}/q_{out})_{ss} = nL\langle \Delta h_{ss} \rangle / rL = nL^2/3Kh_i = L^2/3D \approx 13.8$ days allows to calculate the recharge-induced rise of the aquifer water level over time via Eq. (13).

The rational approximation advanced above is acceptable in this case because the effect of the recharge on the flow is small. This is verified by comparing the results calculated without recharge and with $r = 1.2 \times 10^{-8}$ m/s ≈ 1 mm/day (0.0034 ft/day) shown in Fig. 5. The timing of the hydrographs is excellent in both cases. In the recharge case, the overall match between measured and calculated hydrographs is very good, being excellent on the rising limbs and very good on the falling limbs; the calculated peaks underestimate only slightly the measured ones.

It is clear, however, that considering the recharge isolated from the aquifer's response to it is an approximation. This one-way view of the process ignores that the recharge-induced rise of the aquifer water table reduces the gradient between stream and aquifer, the effect of which is to diminish the transfer of stream water to the aquifer; this leads in turn to lower aquifer depths, relative to the one-way process. Accordingly then, a still higher value than $r = 1.2 \times 10^{-8}$ m/s ≈ 1 mm/day would be more appropriate, which the shape of $\Delta h_{ss}(x)$, Eq. (14), justifies as well. This parabolic profile gives below-average values in the (monitored) near-stream region compared to the average correction $\langle \Delta h_{ss} \rangle$. However, further empirical refinement of the recharge estimate is incongruent with this approximate analysis.

Nevertheless, this performance of the model is remarkable, given its calibration on the artificial, high frequency event of October–November 1989. The validation test is indeed arduous because of the disparate dissipation rates of the two waves. For example, the simulation of the March–April 1990 low-frequency transient yields hydrograph peaks at $x = 100$ m and $x = 200$ m of over 4 ft and at 3 ft, respectively (measured above the initial level). In other words, at the midpoint of the aquifer, the wave maintains 50% of the signal's amplitude, compared to less than 2% for the simulation of the October–November 1989 event. The model's behaviour appears robust, in view of such different dissipation rates. And simulation accuracy would have been even better had a more typical, lower-frequency signal been used for calibration; in that case, a more suitable h_0-value could have been gauged rationally and simply, e.g. by relating it to the magnitudes of the calibration and validation signals.

Bank storage

The water exchange across the stream–aquifer interface can profoundly impact in-stream processes, of which the following are among the most prominent in applied hydrology. Flood wave propagation: attenuation of the peak, via bank storage, and lengthening of the tail, upon water release from storage (Perkins and Koussis, 1996); maintenance of (base) flow in gaining streams during dry periods [Sophocleous et al. (1995) analyse the factors affecting the flow exchange in the context of streamflow depletion and the administration of water rights]; deterioration of stream water quality from contaminated aquifer discharges (Squillace, 1996).

Bank storage is defined as the time integral of the flow rate at the stream–aquifer interface. Alternatively however, bank storage can be calculated from the integral over the aquifer length of the differences of the depth profiles at various times relative to the initial one, which gives the evolution of the water volume in the aquifer relative to

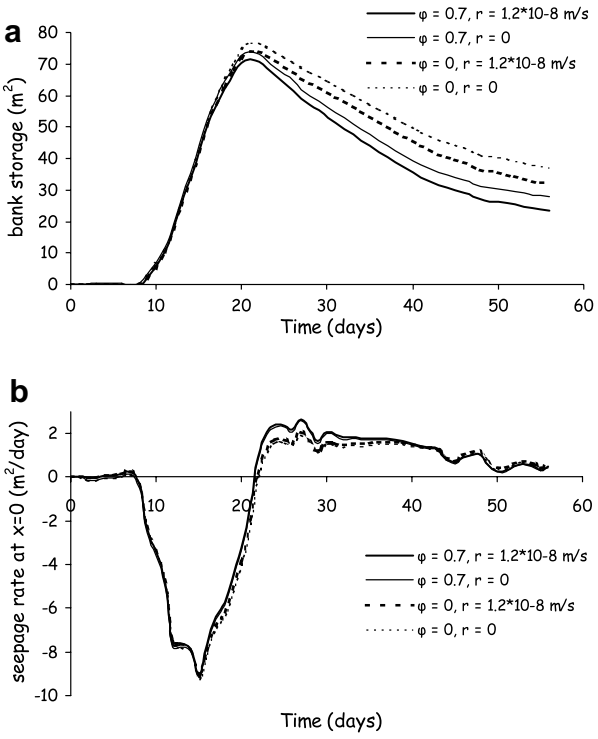

Figure 6 March–April 1990 event simulation, with and without recharge $r = 1.2 \times 10^{-8}$ m/s ≈ 1 mm/day (0.0034 ft/day) and taking the aquifer as sloping and as horizontal: (a) bank storage and (b) seepage rate at the stream–aquifer interface.

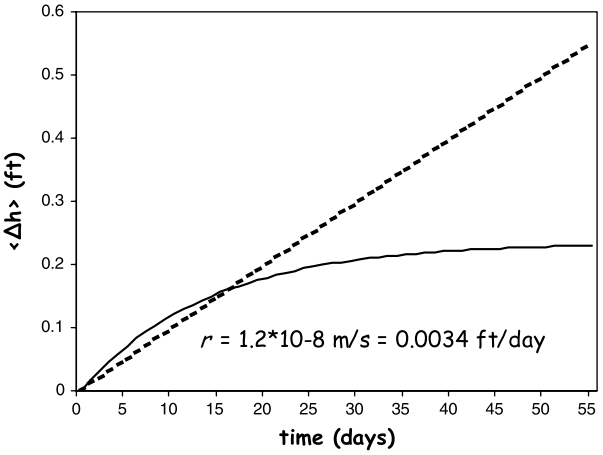

Figure 7 Correction for aquifer rise: 'constant rise' concept with $r = 0.002$ ft/day (dashed line) and linear reservoir concept with $r = 0.0034$ ft/day (solid line).

the initial volume. The modelling should, of course, account for the recharge; else the bank storage would be overestimated. But recharge forcing has not been considered in the analytical solution; therefore an approximation that effects the reduction of the gradients between stream and aquifer is necessary, in order to bring the transfer of stream water to the aquifer closer to reality. The correction consists in lowering the stream stage by an amount equal to the recharge-induced aquifer rise of Eq. (13); with $\langle \Delta h_{ss} \rangle = 0.072$ m and $k = 13.8$ days, this simple correction reduces the gradient at the stream–aquifer interface and thus curtails the water transfer.

The bank storage graphs in Fig. 6a are for flow with and without recharge; Fig. 6b depicts the corresponding seepage rates at the stream–aquifer interface. The value of maximum bank storage is 71.5 m^3/m (73.95 m^3/m without recharge), compared to 58 m^3/m for the numerical MODFLOW model (Squillace, 1996) and 64 m^3/m for the analytical 2D model of Barlow et al. (2000). The maximum value of the seepage rate at the stream–aquifer interface is 9 m^2/day for the 1D model and 7.5 m^2/day for the 2D, both much larger than the MODFLOW simulation's 5.5 m^2/day. For completeness, we add the results for the horizontal aquifer model: maximum bank storage 74.05 m^3/m (76.7 m^3/m without correction for recharge) and maximum seepage rate 9.2 m^2/day, which are slightly inferior (~4%) to the sloping-base model with $\varphi \approx 0.7°$.

As discussed in the case of the leakance, the complete stream penetration assumed in the analytical models underestimates flow resistance. This shortcoming leads to high values of bank storage (relative to the MODFLOW results), against which Hooghoudt's equivalent depth (Van Schilfgaarde, 1970) and Scherer's (1973) added resistance concepts could be used.

The differences between the 1D and 2D model results should be attributed mainly to the linearised nature of the 1D (Dupuit–Forchheimer) model versus the exactly linear 2D model. Apparently, the linearisation makes the diffusive fluxes too large, an effect that is not balanced adequately (small slope) by the gravity-driven counter flux towards the stream, despite the large depths in the near-stream aquifer region. Conceivably, treating the slope as a calibration parameter might improve bank storage and seepage rate results, but model optimisation will become more tedious. In any event, the size of the discrepancy between the two solutions for bank storage and seepage rate surprises, given that both models fit the head data very well and that bank storage is computed from the change of aquifer depth.

Another, but minor reason for the discrepancies is the, over time, larger rise of the water table in the 2D model, due to its use of the 'constant rise' concept for the recharge (accretion); Fig. 7 shows that Eq. (13), with Eq. (15) for $r = 0.0034$ ft/day, and $\langle \Delta h \rangle = rt/n$ for $r = 0.002$ ft/day give about the same values for $t < 20$ days, but deviate strongly thereafter. (Fig. 7 should elucidate our previous comment more, that Barlow et al. (2000) adopted a constant rate of water level rise with $r = 0.002$ ft/day and the attendant overestimation, especially of the falling hydrograph limbs; with the improved recharge correction of Eq. (13) and for $r = 0.0034$ ft/day, the 2D model would probably give aquifer stages very close to the 1D model's.)

Analytical modelling

The stream hydrograph is approximated analytically in the interval 7 days $\leqslant t \leqslant$ 28 days by Eq. (3), with $f = 1 - \cos\omega t$, $A = 25$ ft (7.62 m), $\delta = 0.11$ day^{-1} and $T = 30$ days ($\omega \approx 0.21$ day^{-1}). In fitting Eq. (3) to the data, the time axis is reset such that the origin of the hydrograph is shifted by 7 days; the wave values are above the initial stage 672.8 ft aMSL. The stream hydrograph is seen in Fig. 8a to be approximated well (RMSE ≈ 0.2 ft) over the main interval of the transient. Fig. 8 depicts the convolution solution, with parameters as in the validation case, i.e., as calibrated numerically on the event of October–November 1989, except for $h_0 \cos\varphi = 11.5$ m, and with recharge included as explained above. The results are acceptable over the main body of the transient. The solution for the analytical stream signal, for an aquifer with a base sloping toward the stream and for the case with a low-conductivity sediment bed layer is as follows:

$$h(x,t) = -Ae^{ax} \sum_{v=1}^{\infty} \frac{s_v z_v \left[a \sin(z_v x/L - z_v) + \frac{z_v}{L} \cos(z_v x/L - z_v)\right] e^{s_v t}}{\left(a^2 + z_v^2/L^2\right)\left[\sin z_v (2lz_v + Lz_v - 2laLz_v) + \cos z_v (lz_v^2 + a^2L^2 + 2laL - la^2L^2 - L)\right]} \times \left(\frac{1 - e^{-(s_v+\delta)t}}{s_v} - e^{-(s_v+\delta)t} \frac{-(s_v+\delta)\cos(\omega t) + \omega \sin(\omega t)}{\omega^2 + (s_v+\delta)^2} - \frac{(s_v+\delta)}{\omega^2 + (s_v+\delta)^2} \right). \quad (16)$$

Maximum bank storage of 74.9 m^3/m is comparable to the numerically computed 73.9 m^3/m, without recharge correction; maximum seepage rate is 8.3 m^2/day. Unlike the numerical case, correction due to increased aquifer levels is not possible, as the stream signal must have the specified analytical form. This exercise demonstrates that analytical convolution of periodic or other functions (e.g., linear or exponential), is not only suitable for theoretical work, but has practical utility as well. In particular, efficient convolution of periodic functions can prove useful in combination with Fourier decomposition of the stream signal.

Discussion, summary and conclusions

Solutions for the interaction of a stream with a sloping unconfined aquifer that it fully penetrates were developed, using the SRF of the linear Boussinesq equation in the convolution integral, also taking into account a low-conductivity streambed layer. When the flow-inducing stream stage variations are common functions, these solutions give ana-

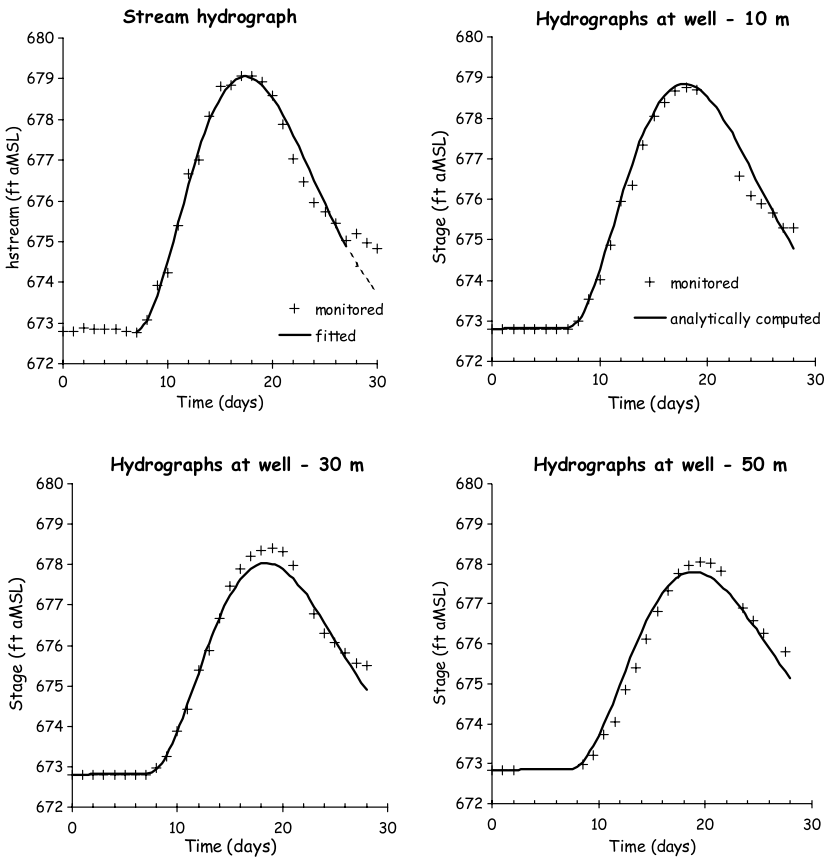

Figure 8 Analytical approximation of the stream hydrograph and variation of the water level in the partially penetrating wells near the stream bank for the March–April 1990 event and analytical model results: crosses, monitored data; solid line, analytically fitted or computed results.

lytically the aquifer stage and flow rate, the flow exchange rate at the stream–aquifer interface and the exchanged volumes; otherwise the convolution is evaluated numerically. The model was first verified on the classical Cooper and Rorabough problem. The responses of aquifers, inclined at $\varphi = \pm 2.5°$ and $\varphi = 0°$, to a periodic change of stream stage demonstrate that the flows in the sloping and the horizontal aquifers, with identical hydraulic properties, can differ noticeably.

Analytical and numerical convolution-derived solutions were used to model the interaction of Cedar River and its adjacent unconfined aquifer near Cedar Rapids, Iowa. In the model, the aquifer base was taken to be horizontal or inclined, and the streambed clogged by a low-conductivity sediment layer. The model was verified against data not used in the calibration. The new 1D model performed very well, giving excellent reproduction of the monitored hydrographs at three monitoring wells. Even though the slope of the aquifer base is small, $\varphi \approx 0.7°$, this field case showed that accounting for the base slope enhances accuracy. The concept of a linear reservoir was employed, in conjunction with an approximate hydraulic analysis, to estimate the influence of recharge in the validation case; the calculations confirmed the rate determined by a numerical simulation with the MODFLOW model. Compared to the results of the exactly linear 2D model, with Stehfest inversion (Barlow and Moench (1998); Barlow et al. (2000)), the bank storage and seepage rate were higher by ~10% and ~15%, respectively. The Cedar River application showed the linearised 1D model's capacity to deal with non-linearity by rational adjustment of the linearisation level. Generally, as long as the interest is in estimating the aquifer's macro-hydraulic response, the 1D model can give useful results.

The successful simulation of the stream–aquifer interaction by the new 1D model as well as by the 2D model of Barlow et al. (2000) calls for a discussion. Both models have three free parameters for calibration: (i) 1D model: the diffusivity, the leakance, and the velocity and (ii) 2D model: the horizontal hydraulic conductivity, the leakance, and the anisotropy ratio of vertical to horizontal conductivity. The base of the equivalent aquifer is not subject to calibration; it is defined after evaluation of the geology of the site, either through its slope or via the initial aquifer depth, which positions the horizontal base of the equivalent aquifer.

The 2D model's higher dimensionality makes it principally superior to the 1D model. Yet, for that innate advantage to become tangible, that model should take the 2D nature of flow into account explicitly. The results of the two models are expected to deviate there where the pressure in the water column is non-hydrostatic (curved streamlines). Thus, considering head variations in the vertical benefits modelling fidelity, where the streamlines curve significantly. Such is the case near a partially penetrating

streambed; yet, by assuming that the stream penetrates the aquifer fully, the 2D model looses its potential advantage. Another reason for the similarity of the computed heads is that the water pressure equilibrates near the static value inside a monitoring well with a long perforation; this is in essential agreement with the Dupuit—Forchheimer hypothesis underpinning the 1D model. Generally, as long as we are interested in the aquifer's macro-hydraulic response (depth, bank storage and flow rate), the 1D model can be useful. On the other hand, the exactly linear 2D model is appropriate, indeed necessary, if a 2D flow field is needed, say, for a more realistic simulation of mass transport in the aquifer.

Acknowledgement

We thank P.M. Barlow of the United States Geological Survey for gracefully providing us the data of the field test at Cedar River alluvial aquifer near Cedar Rapids, Iowa.

References

Akylas, E., Koussis, A.D., submitted for publication. Response of sloping unconfined aquifer to stage changes in adjacent stream: I. Theoretical analysis and derivation of system response functions, J. Hydrol., doi:10.1016/j.jhydrol.2007.02.021.

Barlow, P.M., Moench A.F., 1998. Analytical solutions and computer programs for hydraulic interaction of stream—aquifer systems. US Geological Survey Open-File Report 98-415A, pp. 85.

Barlow, P.M., DeSimone, L.A., Moench, A.F., 2000. Aquifer response to stream-stage and recharge variations. II. Convolution method and applications. Analytical step-response functions. J. Hydrol. 230, 211—219.

Cooper Jr., H.H., Rorabough, M.I., 1963. Ground-water movements and bank storage due to flood stages in surface streams. US Geological Survey Water-Supply 1536-J, pp. 343—366.

Crank, J., 1975. The Mathematics of Diffusion, second ed. Clarendon Press, Oxford.

Hantush, M.S., 1965. Wells near streams with semiprevious beds. J. Geophys. Res. 70 (12), 2829—2838.

Moench, A.F., Barlow, P.M., 2000. Aquifer response to stream-stage and recharge variations . I. Analytical step-response functions. J. Hydrol. 230, 192—210.

Perkins, S.P., Koussis, A.D., 1996. A stream—aquifer interaction model with diffusive wave routing. J. Hydraul. Eng. 122 (4), 210—219.

Rötting, T.S., Carrera, J., Bolzicco, J., Salvany, J.M., 2006. Stream-stage response tests and their joint interpretation with pumping tests. Ground Water 44 (3), 371—385.

Scherer, B., 1973. Die Entwicklung und Anwendung eindimensionaler Modelle der zweidimensionalen Grundwasserbewegung in Fluss-, Graben- und Draennaehe, Technischer Bericht Nr. 9, IHH, Technische Hochschule Darmstadt.

Sophocleous, M.A., 2002. Interactions between groundwater and surface water: the state of the science. Hydrogeol. J. 10 (1), 52—67.

Sophocleous, M., Koussis, A.D., Martin, J.L., Perkins, S.P., 1995. Evaluation of simplified stream—aquifer depletion models for water rights administration. Ground Water 33 (4), 579—588.

Squillace, P.J., 1996. Observed and simulated movement of bank-storage water. Ground Water 34 (1), 121—134.

Squillace, P.J., Caldwell, J.P., Schulmeyer, P.M., Harvey, C.M., 1996. Movement of agricultural chemicals between surface water and ground water Lower Cedar River Basin, Iowa, US Geological Survey Water-Supply Paper 2448, 59pp.

Tóth, J., 1963. A theoretical analysis of groundwater flow in small drainage basins. J. Geophys. Res. 68, 4785—4812.

Van Schilfgaarde, J., 1970. Theory of flow to drains. Adv. Hydrosci. 6, 43—106.